

Spatial distribution of soil moisture in a small catchment. Part 1: geostatistical analysis

A. Bárdossy^{a,*}, W. Lehmann^b

^a*Institut für Wasserbau, Universität Stuttgart, 70550 Stuttgart, Germany*

^b*Institut für Hydrologie und Wasserwirtschaft, Universität Karlsruhe, 76128 Karlsruhe, Germany*

Received 3 June 1997; accepted 24 November 1997

Abstract

Soil moisture measurements were performed weekly at about 60 locations in a small catchment (6.3 km²) in southwest Germany over a period of 6 years. The measurements were carried out by using time domain reflectometry at four different depths. The data was analyzed and a time independent semivariogram was derived. For interpolation, five different methods, ordinary kriging, external drift kriging, indicator kriging, external drift indicator kriging and Bayes–Markov updating were used. Additional information such as topographical parameters derived from a digital elevation model, were used to improve the estimation in the external drift methods. In the Bayesian case, even qualitative information such as land use could be used. Depending on the assumptions, the interpolated maps differed significantly. The performance of the different methods was compared using a cross-validation approach. The results indicate improvement in the interpolation quality by using the topographic index or land use as additional information. © 1998 Elsevier Science B.V. All rights reserved.

Keywords: Geostatistics; Kriging; Soil moisture; Topography

1. Introduction

Soil moisture plays a central role in hydrology. It influences infiltration and runoff processes, as the hydraulic conductivity and the water uptake capacity of the soil during rainfall events is partly determined by the soil moisture content. It is a vital factor in plant evapotranspiration and thus also an important factor for the energy budget in meteorology.

At present, soil moisture can be measured directly at selected locations by using the gravimetric method. Indirect local measurement techniques such as time domain reflectometry (TDR), enable us to carry out detailed measurement campaigns in small areas.

Remote sensing techniques such as microwave and radar measurements deliver detailed spatial information. The calibration of these methods, however, is still a difficult problem. Therefore results obtained by these methods are usually uncertain.

The goal of this investigation is to study the spatial distribution of soil moisture. The study area is the Weiherbach catchment, situated about 30 km north-east of Karlsruhe and belonging to the hilly Kraichgau region in southwest Germany. Loess layers up to ten meters deep are typical for this region. The 6.3 km² catchment area is mainly intensive farmland with the exception of some farm yards, field roads and forest patches. An overview of the catchment area and the positioning of the most important measurement locations are given in Fig. 1.

* Corresponding author. Tel: 00497116854663; Fax: 497116854681; e-mail: bardossy@iws.uni-stuttgart.de

Since autumn 1989 the Weiherbach catchment served as a testing site for an interdisciplinary scientific project investigating transport processes in a small catchment. The project goals are described in Plate et al. (1991).

To determine the soil moisture content in the catchment, the time domain reflectometry method was used (Topp et al., 1980; Topp et al., 1982). The measurements were carried out with IRAMS 6000 and TRASE 6050 XI of Soilmoisture equipment corp. (Santa Barbara, USA) instruments.

Since 1989 up to 110 measurement plots have been installed in the catchment area where about 60 samples are being taken on a weekly basis totalling over 45 000 single readings by autumn 1995. An overview

of the measurement network is given in Fig. 1. Each of the measurement plots consists of four waveguide pairs (see Fig. 2). The measurement depths of 0–30 cm, 0–45 cm and 0–60 cm are permanently installed while the depth 0–15 cm is set every day of the measurement. As mentioned by Topp et al. (1982), it is possible to determine the soil moisture content of different soil layers by using the neighboring measurement depths. As the measured volume of two waveguide pairs is different, such an approach is subject to some problems. To be able to estimate the accuracy of the kriging methods, only direct measurements have been used.

This paper is organized as follows: In Section 2 the spatial variability of soil moisture is investigated by using time invariant variograms. Different geostatistical

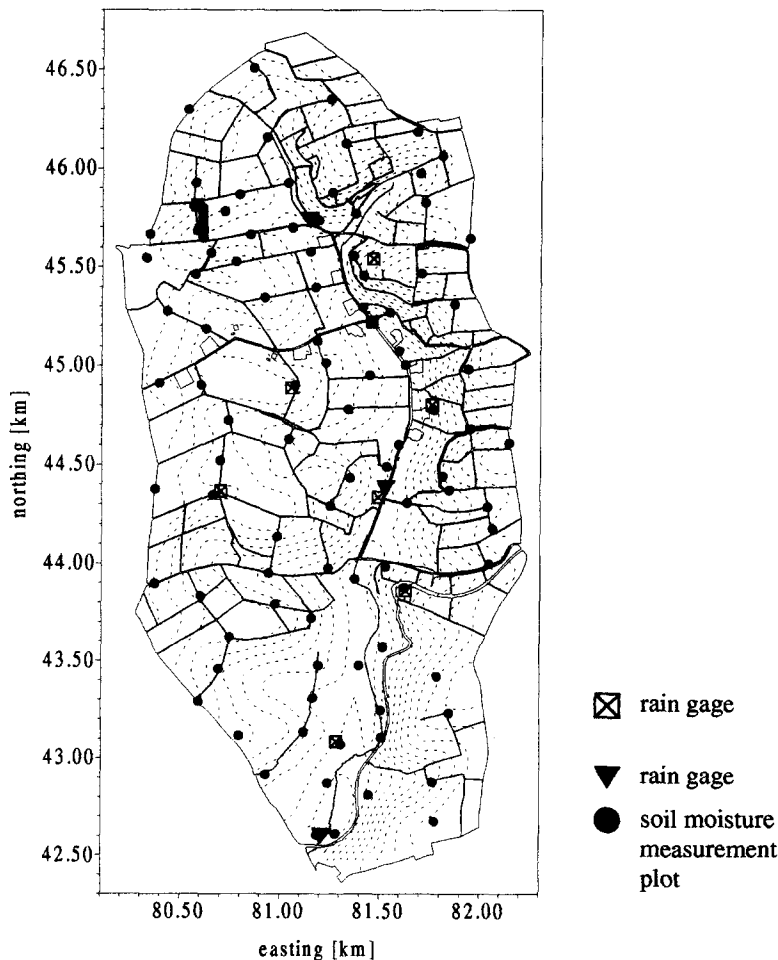


Fig. 1. Location of the observation points in the Weiherbach catchment.

interpolation techniques are described and applied to selected cases in Section 3. The cross-validation comparison of the methods is described in Section 4. Finally the results are summarized, discussed and conclusions are drawn. In the second part of this paper the importance of the different influencing factors is investigated.

2. Spatial variability of soil moisture

Several studies have shown that the water content of the upper soil layers is highly variable both in space and time. (Anderson and Burt, 1977; Anderson and Burt, 1978a; Anderson and Burt, 1978b; Dunne, 1980; Chorley, 1980; Moore et al., 1988; Wood et al., 1990; Kirkby, 1993; Barling et al., 1994). This variability is partly due to the variability of meteorological conditions (precipitation, radiation, temperature), soil properties and vegetation. As a first step the spatial variability was investigated by using variograms.

2.1. Variogram assumptions

In a geostatistical analysis, variograms can be estimated for each realization, in this case for each measurement time and depth separately. This is a rather lengthy procedure, especially considering that there are more than 800 realizations. As time series are available at each point, one could use the calculated co-variances directly, in the same way Schiffler and Bárdossy (1991). Another possibility would be the use of the spatial dispersion function (Montestiez et al., 1993). A simpler approach, the assumption of a time invariant variogram (up to a multiplicative factor) was used in this paper.

A time invariant normed variogram was selected as follows. Suppose the variogram at time t is defined as:

$$\begin{aligned} \gamma_t(h) &= \text{Var}_x[Z(x+h, t) - Z(x, t)] \\ &= \frac{1}{2} E[(Z(x+h, t) - Z(x, t))^2] \end{aligned} \quad (1)$$

It is assumed that a common variogram $\gamma(h)$ exists such that:

$$\gamma_t(h) = \text{Var}_x[Z(x+h, t) - Z(x, t)] = \text{Var}_x[Z(x, t)] \gamma(h). \quad (2)$$

$\text{Var}_x[Z(x, t)]$ denotes the variance of Z at a fixed time t . It was assumed that the variogram at time t is the same as at t' up to a constant multiplier, proportional to the ratio of the variances. This assumption simplifies the calculation of the experimental variogram. The fit of a theoretical curve to assess $\gamma(h)$ has only been performed once.

2.2. Experimental variograms

The time invariant experimental variogram $\gamma^*(h)$ can be estimated by:

$$\gamma^*(h) = \frac{1}{I} \sum_{i=1}^I \frac{\gamma_{t_i}^*(h)}{\text{Var}_x[Z(x, t_i)]}, \quad (3)$$

$\gamma_{t_i}^*(h)$ being the experimental variogram estimated from the data $Z(x, t_i)$ measured at time t_i :

$$\gamma_{t_i}^*(h) = \frac{1}{2N(h)} \sum_{x_l - x_k \approx h} (Z(x_l, t_i) - Z(x_k, t_i))^2. \quad (4)$$

The experimental variograms were calculated for different directions but no anisotropy could be found. Fig. 3 shows the variogram cloud of the normed experimental curves and the universal variogram as defined in Eq. (3). This experimental curve has the

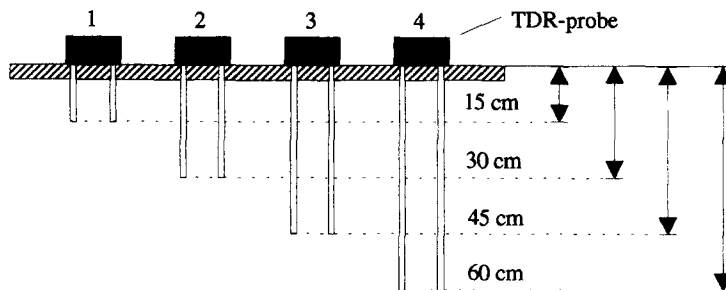


Fig. 2. Measurement plot.

typical shape of a variogram with an increase until 300 m and a sill. This variogram was fitted by a spherical theoretical curve with a nugget and used for subsequent analysis.

Sensitivity analysis was carried out to investigate the effect of a possible error in the variogram parameters. The estimations were quite robust within a reasonable range of parameters. The range had the most important effect on the estimation, but even then the differences were below 5%. Therefore, the estimated values would not differ much using different variograms for each season.

3. Interpolation

After the variogram estimation, the interpolation between the measurement points was carried out. For this purpose different geostatistical methods were used to interpolate a great number of soil moisture maps. The calculation was done for a quadratic grid with 12.5 m grid size. Each map consisted of about 58 000 data points. The soil moisture maps be presented here are based on measurements that were taken on April 8th 1991, at a depth of 0–15 cm. For

this particular day 63 values were obtained. The last rainfall event occurred approximately 1 week before the measurements. At this early time of spring the influence of evaporation on the the soil moisture distribution was expected to be low.

3.1. Ordinary kriging (OK)

OK is the most widely used geostatistical interpolation method (Matheron, 1971). Supposing that the expected value of Z is constant in the whole domain at a given time t :

$$E[Z(x, t)] = m(t), \tag{5}$$

the linear estimator;

$$Z^*(x, t) = \sum_{i=1}^n \lambda_i Z(x_i, t) \tag{6}$$

which minimizes the estimation variance can be found by solving the kriging system:

$$\sum_{i=1}^n \lambda_i \gamma_i(x_j - x_i) + \mu = \gamma_j(x_j - x) \quad j = 1, \dots, n$$

$$\sum_{i=1}^n \lambda_i = 1 \tag{7}$$

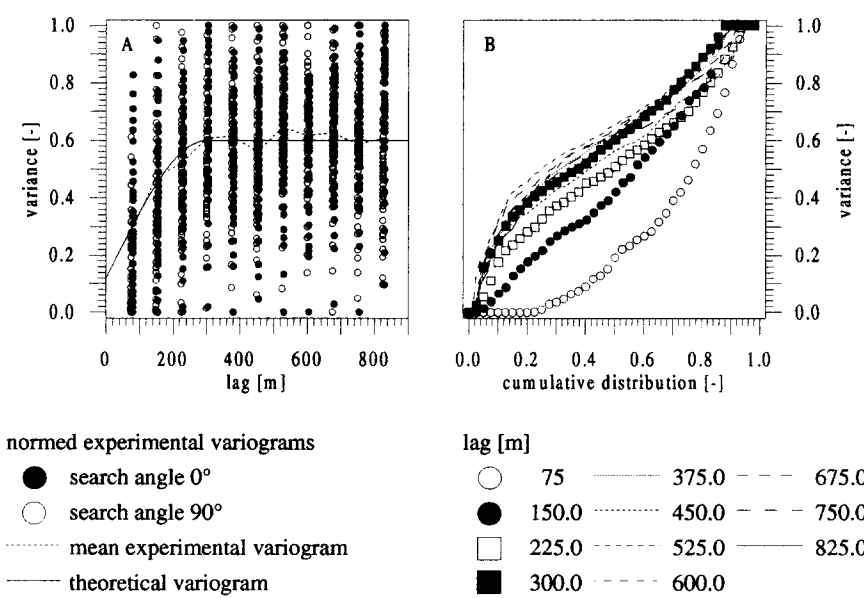


Fig. 3. The variogram cloud and the mean variogram values for the estimation of $\gamma(h)$ based on the time series of 1989–1994. Class: 75 m; search angle ϕ : 0° and 90° ; tolerance δ : 45° ; depth: 0–15 cm. Normalized experimental variograms for two directions: (a) mean experimental variogram, theoretical variogram; (b) relative distribution functions of the normed experimental variograms in different ranges (b).

Note that the weights λ_i remain the same if the time specific variogram γ , is replaced by the time invariant variogram γ assuming Eq. (3).

Fig. 4 shows the map obtained by OK for the selected day. Circular patterns of the map are typically

produced by this method. The influence of measurement points declines with increasing distance to the point, although some terrain structures are recognizable. The valley bottom, for example, especially the small forest that is located at the southern end of the

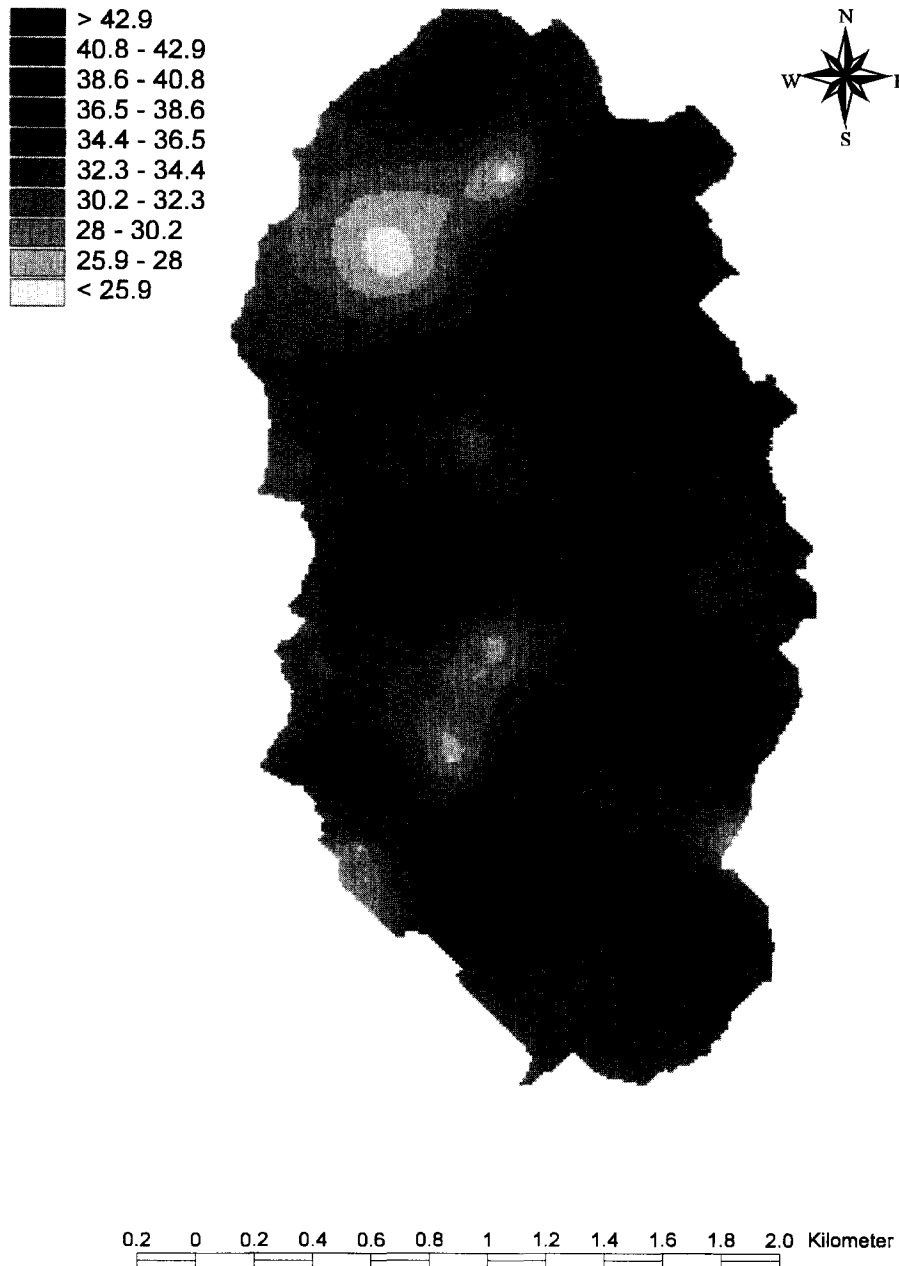


Fig. 4. Soil moisture distribution obtained using OK.

map, is noticeable because of the significantly higher soil moisture values. This can also be said of some of the side valleys. Some of the western hilltops are outlined by low soil moisture values. The pattern of the map differs from what one would expect. The reason for this is that OK neglects the specific properties of the studied variable. In this case even the fact that water only moves downhill has not been considered.

3.2. External drift kriging (EDK)

As described above, the maps of soil moisture distribution obtained by OK show deficiencies. This is partly due to the fact that the method does not consider any physical knowledge corresponding to soil water dynamics. This kind of external knowledge can be incorporated into the system with EDK (Ahmed and De Marsily, 1987). Here it is supposed that an additional variable $Y(x)$ that is linearly related to $Z(x)$ exists. The assumption of the constant expected value is thus replaced by;

$$E[Z(x, t)|Y(x)] = a(t) + b(t)Y(x), \quad (8)$$

where a and b are unknown constants. The linear estimator (Eq. (6)) should be unbiased for any $a(t)$ and $b(t)$ values. Minimizing the estimation variance under this assumption leads to the linear equation system:

$$\sum_{i=1}^I \lambda_j \gamma_i(x_j - x_i) + \mu_1 + \mu_2 Y(x_j) = \gamma_i(x_j - x) \quad (9)$$

$$j = 1 \dots I$$

$$\sum_{i=1}^I \lambda_i = 1$$

$$\sum_{i=1}^I \lambda_i Y(x_i) = Y(x)$$

where μ_1 , and μ_2 are Lagrange-multipliers. The variogram used in Eq. (9) is the same time invariant curve used in OK. To perform an estimation the variable, Y has to be known at the location x . The estimator thus depends on the additional variable $Y(x)$. For this variable, time invariant parameters derived from the digital elevation model were considered.

EDK is an alternative to Cokriging. The reason for using EDK is that as well as additional information $Y(x)$, topographic variables available on a regular grid can be used. Cokriging would require the estimation of covariograms. This could be done at each individual time step or as a time invariant model by

the method described in the previous section. The first method would cause tremendous work. The assumption of a time invariant covariogram was rejected as the soil moisture could be influenced differently at different times. The influence of the additional variable Y (for example topography) in summer is not the same as in winter, thus the covariograms might also differ. This does not influence EDK as $a(t)$ and $b(t)$ are not specified and the external drift is considered as a 'filter'.

The parameter $\ln(a/\tan\beta)$ will now be used to demonstrate how EDK can provide more realistic soil moisture maps (see Fig. 5). This parameter is a combination of slope angle β and local catchment area a . It takes into account how much surface runoff water can reach a certain point in the catchment and whether it can infiltrate at that point or routed to the next point. It was introduced by Beven and Kirkby (1979) as part of TOPMODEL, a distributed rainfall runoff model and is known as a topographic index.

The strong relationship between the soil moisture distribution and the catchment topography is remarkable. Note that in the case of no relationship between the soil moisture Z and the topographic index Y the external drift kriging method would give results very similar to OK. The Weiherbach stream and its contributing creeks, as well as the intermediate hilltops are expressed by different soil moisture values. Even the Kraichbach Creek, into which the Weiherbach distributes at the southwest corner of the area, is partially recognizable. The pattern of the map is finer for OK. Despite this there are still remarkable overlaps with this method, for example at the dry southern end of the map. Compared to OK the influence of extreme measurements is reduced to smaller areas. Inside these areas the influence is higher as can be seen at the two points situated in the forested area, for example. In this region high moisture gradients occur which can exceed physically feasible values. This problem can be investigated mainly in regions where the measured value and the additional parameter are extreme. Wide parts of the map are not influenced by this problem. Here the advantages that can be seen in the finer structure of the map are evident when compared with OK.

3.3. Indicator kriging (IK)

A visible problem both with OK and EDK is that the minima and maxima of the estimated values might

represent a wider range than the observed ones leading to unrealistic high and low estimated values of soil moisture content. One can overcome this problem by using an indicator coding (Journel, 1983).

The indicator variable I_α for a given threshold α is

defined as:

$$I_\alpha(x, t) = \begin{cases} 1 & \text{if } Z(x, t) \leq \alpha \\ 0 & \text{if } Z(x, t) > \alpha \end{cases} \quad (10)$$

The indicator variable I_α can also be regarded as the

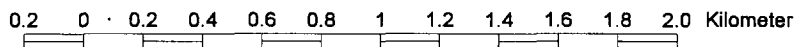
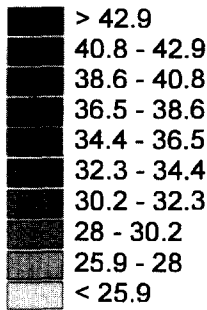


Fig. 5. Soil moisture distribution obtained using EDK.

probability of $Z(x,t)$ being less or equal than α ;

$$I_\alpha(x,t) = P[Z(x,t) \leq \alpha] = F_t(\alpha, x) \quad (11)$$

$F_t(\alpha, x)$ being the distribution function of Z at location x and time t .

If indicator coding is performed for each real value α , then each observation is transformed into a step function. In practice a set of different α_k values $k = 1, \dots, K$ is selected, and $Z(x,t)$ is transformed into the K dimensional vector $(I_{\alpha_1}(x,t), \dots, I_{\alpha_K}(x,t))$

The indicator variables $I_{\alpha_k}(x)$ were defined by dividing the measurement values corresponding to a selected time t into five classes. The classes have been selected between minima and maxima of the measurements with equal numbers of values in each class.

The IK interpolated soil moisture maps is shown in Fig. 6. At first, the map seems to produce a similar pattern as OK (see Fig. 4). A closer look shows some recognizable differences between OK and IK. For example the distribution of soil moisture is more homogeneous. At the northern and southern edge of the map a unification of wet patches took place that went along with a soil moisture reduction. Similar effects appear at formerly dry areas. The terrain structure that was already difficult to see with OK becomes less recognizable. In general it has to be pointed out that this method is a very useful tool to minimize the local effects of extreme measurements, but otherwise suffers from similar problems to OK.

3.4. External drift indicator kriging (EDIK)

IK overcomes the problem of unrealistic values of estimated minima and maxima, but it does not consider additional information as EDK does. A simple extension of the IK can be done by taking an external drift for the indicator variables into account. This leads to the assumption that the 'a-priori' distribution function at location x and time t $F_t(\alpha, x)$ can be written as:

$$F_t(\alpha, x) = E[I_\alpha(x, t) | Y(x)] = a_\alpha(t) + b_\alpha(t)Y(x). \quad (12)$$

Fig. 7 shows an interpolation by EDIK with the additional information $-\ln(a/\tan\beta)$. The map is quite similar to the one of EDK (see Fig. 5). The smoothing effect due to the use of indicator coding can be observed on this figure. The influence of extreme values is reduced, as they are limited within the

range of observations. However some high soil moisture gradients do still exist that can be seen for example at the western part of the map. All in all the structure of the map seems to be more realistic than any of the previous ones.

3.5. Bayes–Markov updating (BMU)

The two previously described procedures EDK and EDIK can consider additional information, but in a numerical form, assuming a linear relationship. However, the soil moisture content is also highly influenced by categorical variables, such as land use or soil type. A non-linear relationship with the additional variable is also possible. An estimation method to cope with these problems is the Bayes–Markov kriging (BMK) described in Zhu and Journel (1993). For this application a simplified form of Bayes–Markov updating (BMU) was used. This differs from BMK by only using the prior information available at the point for which the estimation has to be made. The reason for doing this is that additional information was available at each point of the catchment and little improvement was expected from taking into account further additional information.

Formally BMU uses the assumption that additional information can be taken into account for the assessment of prior distributions at selected locations.

$$U_\alpha(x, t) = P[Z(x, t) \leq \alpha | \text{additional information}]. \quad (13)$$

If this U_α is different from the distribution $F_t(\alpha, x)$ then the additional information is useful for the estimation of $Z(x, t)$. The estimation is then performed by using the global prior $F_t(\alpha, x)$, the local prior $U_\alpha(x, t)$ information and the indicator coded observations $Z(x_i, t)$. For BMU it has to be assumed that $U_\alpha(x, t)$ is available at each location in the domain. The indicator values I_α are estimated using a simple cokriging approach:

$$I_\alpha^*(x, t) = \lambda_0 F_t(\alpha, x) + \sum_{i=1}^n \lambda_i I_\alpha(x_i, t) + v U_\alpha(x, t) \quad (14)$$

In fact BMU is a 'mixture' of three possible approaches:

1. assigning the same mean to the whole domain (λ_0);
2. spatial interpolation ($\lambda_i, i = 1, \dots, n$);

3. assigning the same value to each class of the additional variable v .

The spatial dependence, the configuration of the observation points and the usefulness of the additional information, influence the role of the above factors.

For the calculation of the weights λ_i and v the co-variance function of I_α and U_α and their cross-co-variance function are needed. The formulation of the equations using variograms is also possible, but in this case the co-variance based form is simpler.

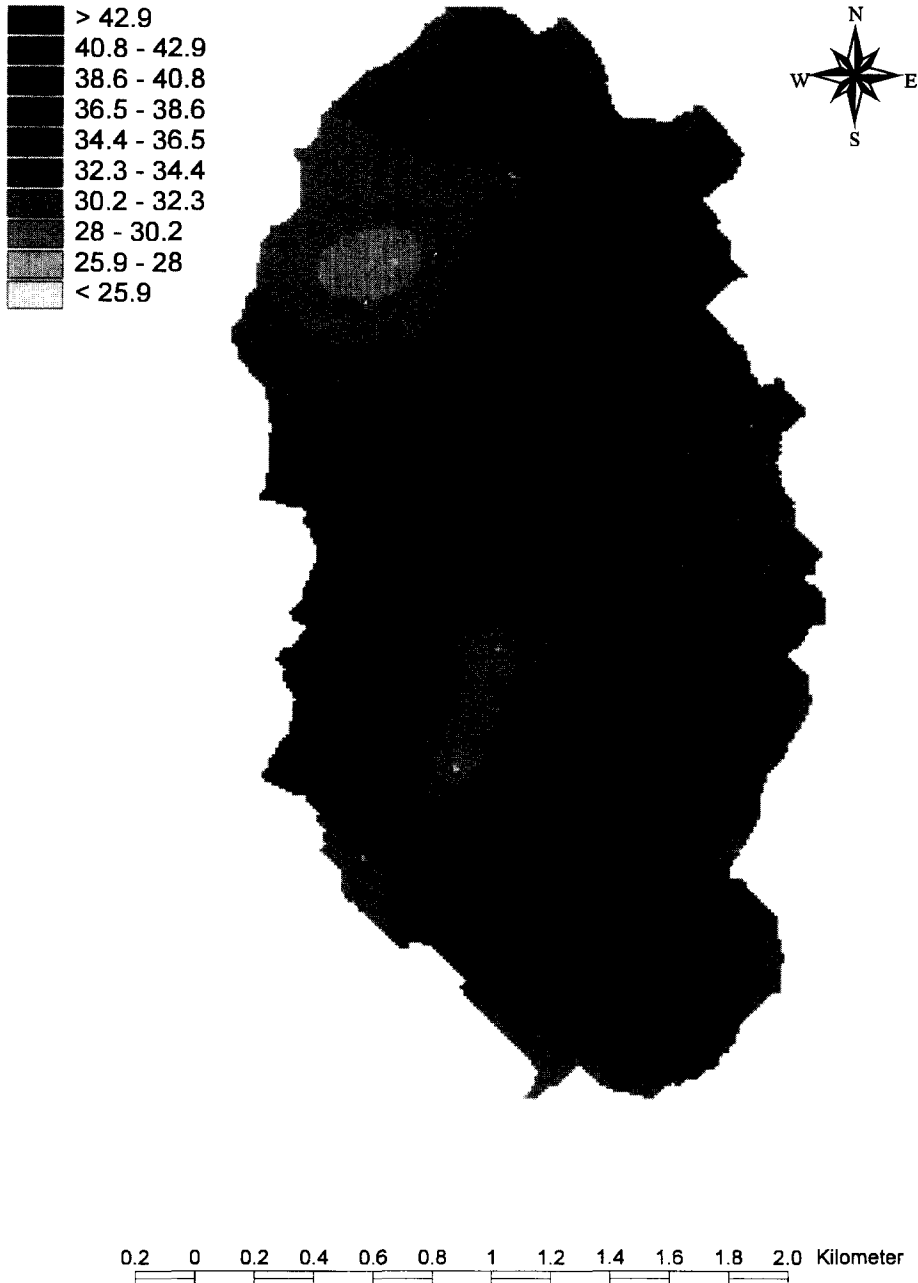


Fig. 6. Soil moisture distribution obtained using IK.

According to Zhu and Journel (1993) the co-variance function of U and the cross co-variance function of I and U can be expressed with the help

of the co-variance function of I .

$$C_{IU}(h) = B(\alpha)C_I(h) \quad (15)$$

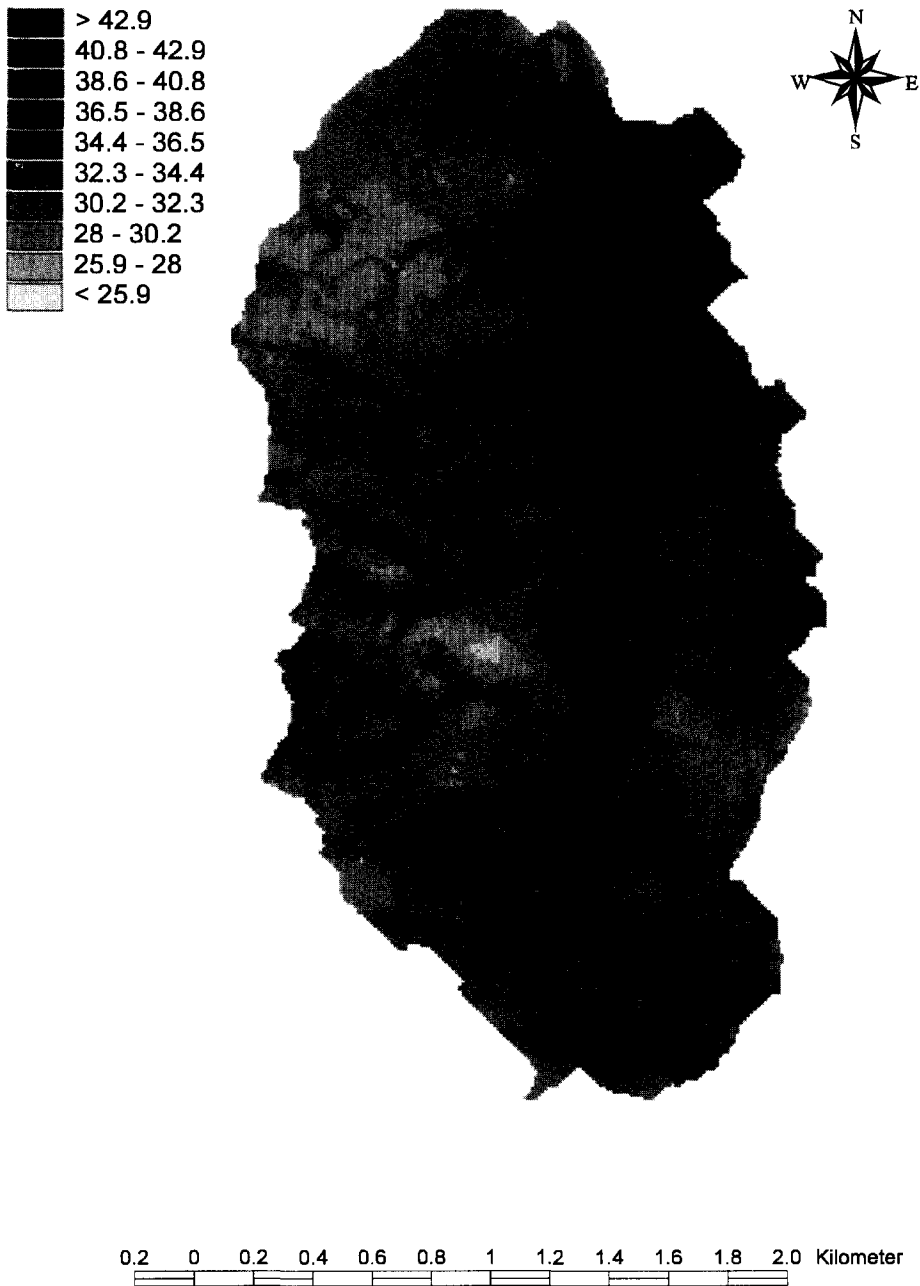


Fig. 7. Soil moisture distribution obtained using EDIK.

and

$$C_U(h) = \begin{cases} B^2(\alpha)C_f(h) & \text{if } h > 0 \\ B^2(\alpha) + V_f^2(\alpha) & \text{for } h = 0 \end{cases} \quad (16)$$

Here the quantities $B(\alpha)$, $V_c(\alpha)$ and $V_f(\alpha)$ reflect the usefulness of the additional information.

They are formally defined as

$$B(\alpha) = E[U_\alpha(x, t) | I_\alpha(x, t) = 1] - E[U_\alpha(x, t) | I_\alpha(x, t) = 0] \quad (17)$$

and

$$V_f^2(\alpha) = F_r(\alpha, x) \text{Var}[U_\alpha(x, t) | I_\alpha(x, t) = 1] + (1 - F_r(\alpha, x)) \text{Var}[U_\alpha(x, t) | I_\alpha(x, t) = 0] \quad (18)$$

The weights λ_i and ν are calculated by using simple cokriging with the single additional point x :

$$\sum_{i=1}^n \lambda_i C_I(x_i - x_j) + \nu C_{IU}(x_j - x) = C_I(x_j - x)$$

for $j = 1, \dots, n$

$$\sum_{i=1}^n \lambda_i C_{IU}(x_i - x) + \nu C_U(0) = C_{IU}(0) \quad (19)$$

One can see from the equation system above that the updating of the prior functions depends on $C_U(0)$ and $C_{IU}(0)$. The bigger the value of $V_f^2(\alpha)$ the higher the importance of the directly measured information. This is reasonable as $V_f^2(\alpha)$ reflects the quality of the additional information.

The additional information $Y(x)$ available at each location x is used to define the variable U_α as

$$U_\alpha(x, t) = \frac{1}{N(x)} \sum_{Y(x_j) \approx Y(x)} I_\alpha(x_j, t) \quad (20)$$

$N(x)$ is the number of observation points which have similar Y values ($Y(x) \approx Y(x_j)$). In practice this is done in the same manner as classes are defined for the variable $Y(x)$ and the mean indicator values over the classes are assigned to the unobserved locations as prior information. Note that $Y(x)$ can be any classification and both numeric values can be grouped into classes or categorical variables, such as land use. The quantities $B(\alpha)$ and $V_f(\alpha)$ can easily be calculated once U_α has been defined.

BMU was performed by using two different additional variables, the topographic index $\ln(a/\tan\beta)$ and land use L .

The structure of the map obtained by BMU (see

Fig. 8) is characterized by the topographic index $\ln(a/\tan\beta)$. In spite of this some changes are recognizable, the structure, for example, is coarser than it appears to be for interpolations with EDK. The effects of extreme measurements are very low. Characteristic centers where such measurements dominate the map do not exist. Large portions of the catchment are characterized by medium soil moistures, where the soil moisture gradients are remarkably low. The map interpolated using BMU is the most realistic soil moisture distribution that has been introduced so far.

The land use L is one of the few parameters that can be used as additional information only by BMU (see Fig. 9).

Different structures that have been introduced before can be found from the map. First in the BMU case, the additional information plays an important role. Taking a closer look, the field borders can be identified by changes in soil moisture and the edge of the land use classification map can also be identified. Regarding the areas that lay outside the classified region, it can be seen that the soil moisture map is not dominated by the additional information. A pattern similar to that of OK or IK can be found mainly in the southwestern corner of the map. This shows that the prior functions do not become effective at points where no improvement in the estimation is expected. The high soil moisture in the forested areas is remarkable. As with the high values in the forest at the southern end, this information spreads over to other areas within this land use class. Thanks to the interpolation within classes, the method is thus able to use information from outside the chosen search range. The example shows that in order to stabilize calculations, a certain number of measurement points is needed, otherwise extreme values will be over-represented. With the exception of forested areas, the soil moisture distribution of the map is quite homogeneous. Areas that appear wet or dry by using other methods can also be identified. However the borders of these areas are greatly influenced by the additional information.

4. Statistical comparison of the results

In the previous sections, examples of interpolated soil moisture maps were shown. As these are very different, statistical comparison is also needed in

addition to a plausibility check. For this purpose split-sampling or jackknife type methods are best suited (Lehmann, 1983). For this application the jackknife approach was selected: for each observa-

tion, the measured value $Z^*(x_j, t_i)$ was compared with the estimated value $Z^*(x_j, t_i)$ obtained by using the other measurements only. Statistics of the differences between these two values were

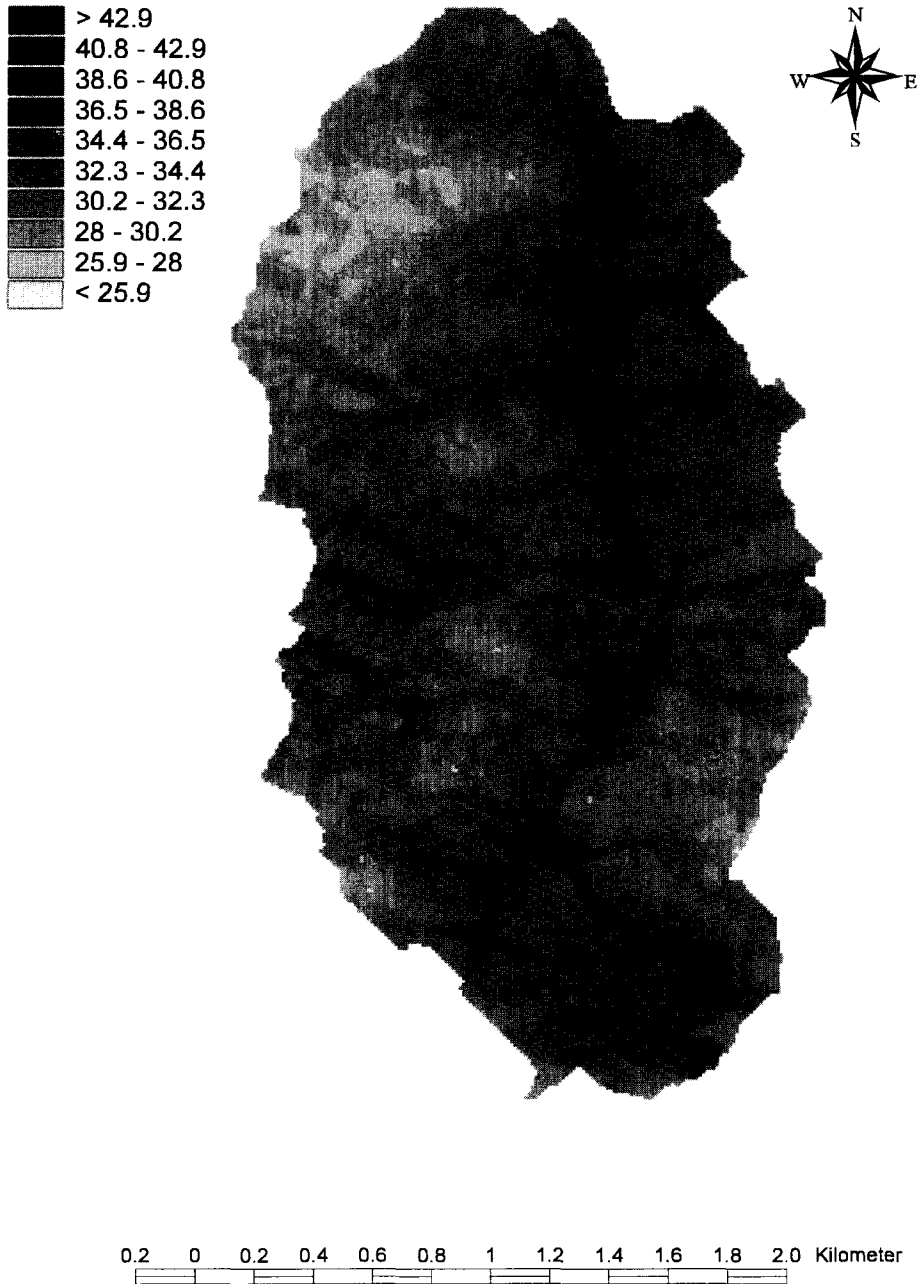


Fig. 8. Soil moisture distribution obtained using BMU and the topographic index $\ln(a/\tan\beta)$.

then carried out. These include the mean error

$$E_1 = \sum_{i=1}^I \sum_{j=1}^J (Z(x_j, t_i) - Z^*(x_j, t_i)) \quad (21)$$

and the mean squared error:

$$E_2 = \sum_{i=1}^I \sum_{j=1}^J (Z(x_j, t_i) - Z^*(x_j, t_i))^2 \quad (22)$$



Fig. 9. Soil moisture distribution obtained using BMU and land use.

This procedure was repeated for each interpolation method and the results were compared. It was assumed for this comparison that one method performs better than another on the entire field, if the test results of the measurement dataset are better. Table 1 shows the results of the comparison for the selected day.

One can see from the table that all the methods are unbiased, the E_1 values are around zero. The additional information improves the interpolation. OK and IK were the 'worst' methods. BMU is the most sophisticated one, but it also yields the best results. The improvement in the squared error is more than 30%. The error measures corresponding to the land use and the topographic index used with the BMU are comparable. Further examples can be found in Lehmann (1995).

5. Discussion and conclusions

From the presented applications the following conclusions can be drawn: kriging methods are useful tools for the regionalization of soil moisture data. The use of additional information allows a physically feasible estimation of the spatial distribution of soil moisture in a catchment area. The chosen 12.5×12.5 m grid size allows a high spatial resolution of the soil moisture maps. As long as parameter characteristics are known, the additional information can be used to transfer interpolation results to other catchments with limited number of data. BMU is a universal tool to regionalize soil moisture as it considers relevant influencing factors. The method allows the use of simple parameters to describe the main hydrological processes that take part in the soil water dynamics. Other potential uses for BMU would be; the analysis of the spatial distribution of air

pollution, rehabilitation of waste disposal sites or determination of ground water maps. Numerical models, geological, topographical or any other type of information can be used as additional variable to assess the soft variable U_α . The computational effort of the OK and EDK is much lower than that of the other procedures, because of the indicator coding, although the estimation of the 58 000 grid points using BMU was performed on a PC without difficulty.

To set out a measurement network which provides representative input data for BMU, a few basic needs have to be considered:

- The influencing factors to be used as additional information have to be known at each measurement and grid point.
- A network of about 50 different points should be set out which takes into account that all classes are represented by points.
- The first measurement data can be used to analyse the geostatistical parameters. The range of the variogram gives the basic information if the distance between the measurement points is close enough.
- With the help of the Jackknife comparison method the measurement network can be optimized. In parts of the catchment area with low estimation errors, the network can be thinned out, in parts with high errors, more points have to be set.
- The procedure has to be repeated a few times until the network can be set out finally to start the measurement campaign.

In summary this paper investigates the application of different geostatistical interpolation techniques to the estimation of soil moisture content. Concluding points may be made as follows:

1. OK is an applicable method, but does not yield physically feasible spatial distributions of soil moisture.
2. EDK with additional topographic information (like $\ln(A/\tan\beta)$) gives very detailed plausible spatial structures, but the estimated values are out of the observation range at some locations.
3. IK results are similar to the ones of OK.
4. EDIK with additional topographic information (such as $\ln(A/\tan\beta)$) gives very detailed plausible

Table 1
Jackknife statistics for the different interpolation methods

Method	E_1 (vol.%)	E_2 (vol.%) ²
OK	- 0.3	32.3
EDK	- 0.2	28.7
IK	- 0.4	29.3
EDIK	- 0.1	26.6
BMU $\ln(a/\tan\beta)$	- 0.1	22.0
BMU L	0.4	22.5

spatial structures and overcomes the range problem of EDK.

5. BMU with topographic additional information (such as $\ln(a/\tan\beta)$) gives physically plausible spatial distributions and also makes the consideration of land use and soil type possible.
6. Two performance indices have been defined to compare the methods.
7. Jackknife comparison of the methods shows that additional information improves the quality of interpolation.

Acknowledgements

Research leading to this paper was carried out as part of the interdisciplinary scientific research program 'Prognosemodell für die Gewässerbelastung aus kleinen ländlichen Einzugsgebieten' which was funded by the German Ministry of Education, Science, Research and Technology (BMBF).

References

- Ahmed, S., De Marsily, G., 1987. Comparison of geostatistical methods for estimating transmissivity using data on transmissivity and specific capacity, *Wat. Resour. Res.*, 23, 1717–1737.
- Anderson, M.G., Burt, T.P., 1977. Automatic monitoring of soil moisture conditions in a hillslope spur and hollow, *J. Hydrol.*, 33, 27–36.
- Anderson, M.G., Burt, T.P., 1978. Toward a more detailed field monitoring of variable source areas, *Wat. Resour. Res.*, 14, 1123–1131.
- Anderson, M.G., Burt, T.P., 1978. The role of topography in controlling throughflow generation, *Earth Surf. Processes*, 3, 331–344.
- Barling, R.D., Moore, I.D., Grayson, R.B., 1994. A quasi-dynamic wetness index for characterizing the spatial distribution of zones of surface saturation and soil water content, *Wat. Resour. Res.*, 30, 1029–1044.
- Beven, K.J., Kirkby, M.J., 1979. A physically based variable contributing area model of basin hydrology, *Hydrol. Sci. Bull.*, 24, 43–69.
- Chorley, R.J., 1980. The hillslope hydrological cycle. In: Kirkby, M.J. (Ed.), *Hillslope Hydrology*, Wiley, Chichester, pp. 1–42.
- Dunne, T., 1980. Field studies of hillslope processes. In: Kirkby, M.J. (Ed.), *Hillslope Hydrology*, Wiley, Chichester, pp. 227–293.
- Journel, A.G., 1983. Non-parametric estimation of spatial distributions, *Math. Geol.*, 15, 445–468.
- Kirkby, M.J., 1993. Long term interactions between networks and hillslopes. In: Beven, K.J., Kirkby M.J., *Channel Network Hydrology*, Wiley, Chichester, 256–293.
- Lehmann, E.L., 1983. *Theory of Point Estimation*, Wiley, New York.
- Lehmann, W., 1995. *Anwendung geostatistischer verfahren auf die bodenfeuchte in ländlichen einzugsgebieten*. Ph.D. thesis, University of Karlsruhe, Karlsruhe.
- Matheron, G., 1971. The theory of regionalized variables and its applications, *Cahiers cent. morph. mat.*, 5, 211.
- Montestiez, P., Sampson, P.D., Guttorp, P., 1993. Modeling of heterogeneous spatial correlation structure by spatial deformation, *Cahiers Geostatist.*, 3, 35–46.
- Moore, I.D., Burch, G.J., Mackenzie, D.H., 1988. Topographic effects on the distribution of surface soil wafer and the location of ephemeral gullies, *Trans. Am. Soc. Ag. Engng*, 31, 1098–1107.
- Plate, E.J., Buck, W., Bronstert, A., Schiffier, G.R., 1991. A multidisciplinary project for modelling transport processes in a small rural catchment. In: *Nachtnebel H.P., Kovar K. (Eds.), Hydrological Basis of Ecological Sound Management of Soil and Groundwater*, IAHS, Wallingford, 61–70.
- Schiffier, G., Bárdossy, A., 1991. Geostatistical assessment of space-time distributed data: application to soil moisture measurements in an experimental catchment. In: *Nachtnebel H.P., Kovar K., (Eds.), Hydrological Basis of Ecologically Sound Management of Soil and Groundwater*, IAHS, Wallingford, 279–287.
- Topp, G.C., Davis, J.L., Annan, A.P., 1980. Electromagnetic determination of soil water content; measurement in coaxial transmission lines, *Wat. Resour. Res.*, 16, 574–582.
- Topp, G.C., Davis, J.L., Annan, A.P., Electromagnetic determination of soil water content using TDR: I: Applications to wetting fronts and steep gradients II: Evaluation of installation and configuration of parallel transmission lines, *Journal of the American Society of Soil science* 49 (1982) 672–678–678–684.
- Wood, E.F., Sivapalan, M., Beven, K.J., 1990. Similarity and scale in catchment storm response, *Rev. Geophys.*, 28, 1–18.
- Zhu, H., Journel, A.G., *Formatting and Integrating Soft Data: Stochastic Imaging via the Markov-Bayes Algorithm*, in: A. Soares (Ed.) *Geostatistics Tróia'92*, Kluwer, Dordrecht, 1993 pp. 1–12.